

# Phenomenology of the radion in the Randall-Sundrum scenario at colliders

Saebiyok Bae, P. Ko, Hong Seok Lee

*Department of Physics, KAIST, Taejon 305-701, Korea*

Jungil Lee

*Luruper Chaussee 149 II, Institut für Theoretische Physik*

*Universität Hamburg, 22761 Hamburg, Germany*

## Abstract

Phenomenology of a radion ( $\phi$ ) that stabilizes the modulus in the Randall-Sundrum scenario is considered. The radion couples to the trace of energy momentum tensor of the standard model (SM) with a strength suppressed only by a new scale ( $\Lambda_\phi$ ) of an order of the electroweak scale. In particular, the effective coupling of a radion to two gluons is enhanced due to the trace anomaly of QCD. Therefore, its production cross section at hadron colliders could be enhanced, and the dominant decay mode of a relatively light radion is  $\phi \rightarrow gg$ , unlike the SM Higgs boson case. We also present constraints on the mass  $m_\phi$  and the new scale  $\Lambda_\phi$  from the Higgs search limit at LEP and perturbative unitarity bound.

PACS numbers :11.10.Kk, 11.25.M

It is one of the problems of the standard model (SM) to stabilize the electroweak scale relative to the Planck scale under quantum corrections, which is known as the gauge hierarchy problem. Traditionally, there have been basically two avenues to solve this problem : (i) electroweak gauge symmetry is spontaneously broken by some new strong interactions (technicolor or its relatives) or (ii) there is a supersymmetry (SUSY) which is spontaneously broken in a hidden sector, and superpartners of SM particles have masses around the electroweak scale  $O(100 - 1000)$  GeV. However, new mechanisms based on the developments in superstring and M theories including D-branes have been suggested by Randall and Sundrum [1]. If our world is confined to a three dimensional brane and the warp factor in the Randall and Sundrum (RS) theory is much smaller than 1, then loop corrections can not destroy the mass hierarchy derived from the relation  $v = e^{-kr_c\pi}v_0$ , where  $v_0$  is the VEV of Higgs field ( $\sim O(M_P)$ ) in the 5 dimensional RS theory,  $e^{-kr_c\pi}$  is the warp factor, and  $v$  is the VEV of Higgs field ( $\sim 246$  GeV) in the 4 dimensional effective theory of the RS theory by a kind of dimensional reduction. Especially the extra-dimensional subspace needs not be a circle  $S^1$  like the Kaluza-Klein theory [1], and in that case, it is crucial to have a mechanism to stabilize the modulus. One such a mechanism was recently proposed by Goldberger and Wise (GW) [2] [3], and also by Csáki et al. [4]. In such a case, the modulus (or the radion  $\phi$  from now on) is likely to be lighter than the lowest Kaluza-Klein excitations of bulk fields. Also its couplings to the SM fields are completely determined by general covariance in the four-dimensional spacetime, as shown in Eq. (1) below. If this scenario is realized in nature, this radion could be the first signature of this scenario, and it would be important to determine its phenomenology at the current/future colliders, which is the purpose of this work. Some related issues were addressed in Ref. [5].

In the following, we first recapitulate the interaction Lagrangian for a single radion and the SM fields, and calculate the decay rates and the branching ratios of the radion into SM particles. Then the perturbative unitarity bounds on the radion mass  $m_\phi$  and  $\Lambda_\phi$  are considered. Current bounds on the SM Higgs search can be easily translated into the corresponding bounds on the radion, which we will show in brief. Then the radion

production cross sections at next linear colliders (NLC's) and hadron colliders such as the Tevatron and LHC are calculated. Then our results will be summarized at the end.

The interaction of the radion with the SM fields at an electroweak scale is dictated by the 4-dimensional general covariance, and is described by the following effective Lagrangian [4] [3] :

$$\mathcal{L}_{\text{int}} = \frac{\phi}{\Lambda_\phi} T_\mu{}^\mu(\text{SM}) + \dots, \quad (1)$$

where  $\Lambda_\phi = \langle \phi \rangle \sim O(v)$ . The radion becomes massive after the modulus stabilization, and its mass  $m_\phi$  is a free parameter of electroweak scale [4]. Therefore, two parameters  $\Lambda_\phi$  and  $m_\phi$  are required in order to discuss productions and decays of the radion at various settings. The couplings of the radion with the SM fields look like those of the SM Higgs, except for  $v \rightarrow \Lambda_\phi$ . However, there is one important thing to be noticed : the quantum corrections to the trace of the energy-momentum tensor lead to trace anomaly, leading to the additional effective radion couplings to gluons or photons in addition to the usual loop contributions. This trace anomaly contributions will lead to distinct signatures of the radion compared to the SM Higgs boson.

The trace of energy-momentum tensor of the SM fields at tree level is easily derived :

$$T_\mu{}^\mu(\text{SM})^{\text{tree}} = \left[ \sum_f m_f \bar{f} f - 2m_W^2 W_\mu^+ W^{-\mu} - m_Z^2 Z_\mu Z^\mu + (2m_h^2 h^2 - \partial_\mu h \partial^\mu h) + \dots \right], \quad (2)$$

where we showed terms with only two SM fields, since we will discuss two body decay rates of the radion into the SM particles, except the gauge bosons of which virtual states are also considered. The couplings between the radion  $\phi$  and fermion pair or weak gauge boson pair are simply related with the SM Higgs couplings with these particles through simple rescaling :  $g_{\phi-f-\bar{f}} = g_{h-f-\bar{f}}^{\text{SM}} v/\Lambda_\phi$ , and so on. On the other hand, the  $\phi-h-h$  coupling is more complicated than the SM  $h-h-h$  coupling. There is a momentum dependent part from the derivatives acting on the Higgs field, and this term can grow up as the radion mass gets larger or the CM energy gets larger in hadroproductions of the radion. It may lead to the violation of perturbative unitarity, which will be addressed after we discuss the decay rates of the radion. Finally, the  $h-\phi-\phi$  coupling could be described by

$$\mathcal{L}_{\text{int}}(h\phi^2) = \frac{v}{\Lambda_\phi^2} \phi^2 \left[ \frac{1}{2} \partial^2 h + \frac{m_h^2}{2} h \right], \quad (3)$$

which might lead to an additional Higgs decay  $h \rightarrow \phi\phi$ , if this mode is kinematically allowed, thereby enlarging the Higgs width compared to the SM case. However, this coupling actually vanishes upon using the equation of motion for the Higgs field  $h$ . This is also in accord with the fact that the radion couples to the trace of the energy momentum tensor and there should be no  $h - \phi$  mixing after field redefinitions in terms of physical fields.

In addition to the tree level  $T_\mu^\mu(\text{SM})^{\text{tree}}$ , there is also the trace anomaly term for gauge fields [6] :

$$T_\mu^\mu(\text{SM})^{\text{anom}} = \sum_{G=\text{SU}(3)_C, \dots} \frac{\beta_G(g_G)}{2g_G} \text{tr}(F_{\mu\nu}^G F^{G\mu\nu}), \quad (4)$$

where  $F_{\mu\nu}^G$  is the field strength tensor of the gauge group  $G$  with generator(s) satisfying  $\text{tr}(t_G^a t_G^b) = \delta^{ab}$ , and  $\beta_G$  is the beta function for the corresponding gauge group. The trace anomaly term couples with the parameter of conformal transformation in our 3-brane. And the radion  $\phi$  plays the same role as the parameter of conformal transformation, since it belongs to the warp factor in the 5 dimensional RS metric [4]. Therefore, the parameter associated with the conformal transformation is identified with the radion field  $\phi$ . As a result, the radion  $\phi$  has a coupling to the trace anomaly term. For QCD sector as an example, one has

$$\frac{\beta_{QCD}}{2g_s} = -(11 - \frac{2}{3}n_f) \frac{\alpha_s}{8\pi} \equiv -\frac{\alpha_s}{8\pi} b_{QCD}, \quad (5)$$

where  $n_f = 6$  is the number of active quark flavors. There are also counterparts in the  $SU(2) \times U(1)$  sector. This trace anomaly has an important phenomenological consequence. For relatively light radion, the dominant decay mode will not be  $\phi \rightarrow b\bar{b}$  as in the SM Higgs, but  $\phi \rightarrow gg$ .

Using the above interaction Lagrangian, it is straightforward to calculate the decay rates and branching ratios of the radion  $\phi$  into  $f\bar{f}, W^+W^-, Z^0Z^0, gg$  and  $hh$ .

$$\Gamma(\phi \rightarrow f\bar{f}) = N_c \frac{m_f^2 m_\phi}{8\pi \Lambda_\phi^2} (1 - x_f)^{3/2},$$

$$\begin{aligned}
\Gamma(\phi \rightarrow W^+W^-) &= \frac{m_\phi^3}{16\pi\Lambda_\phi^2} \sqrt{1-x_W} (1-x_W + \frac{3}{4}x_W^2), \\
\Gamma(\phi \rightarrow ZZ) &= \frac{m_\phi^3}{32\pi\Lambda_\phi^2} \sqrt{1-x_Z} (1-x_Z + \frac{3}{4}x_Z^2), \\
\Gamma(\phi \rightarrow hh) &= \frac{m_\phi^3}{32\pi\Lambda_\phi^2} \sqrt{1-x_h} (1 + \frac{x_h}{2})^2, \\
\Gamma(\phi \rightarrow gg) &= \frac{\alpha_s^2 m_\phi^3}{32\pi^3 \Lambda_\phi^2} \left| b_{QCD} + \sum_q I_q(x_q) \right|^2,
\end{aligned} \tag{6}$$

where  $x_{f,W,Z,h} = 4m_{f,W,Z,h}^2/m_\phi^2$ , and  $I(z) = z[1 + (1-z)f(z)]$  with

$$\begin{aligned}
f(z) &= -\frac{1}{2} \int_0^1 \frac{dy}{y} \ln[1 - \frac{4}{z}y(1-y)] \\
&= \begin{cases} \arcsin^2(1/\sqrt{z}), & z \geq 1, \\ -\frac{1}{4} \left[ \ln\left(\frac{1+\sqrt{1-z}}{1-\sqrt{1-z}}\right) - i\pi \right]^2, & z \leq 1. \end{cases}
\end{aligned} \tag{7}$$

Note that as  $m_t \rightarrow \infty$ , the loop function approaches  $I(x_t) \rightarrow 2/3$  so that the top quark effect decouples and one is left with  $b_{QCD}$  with  $n_f = 5$ . For  $\phi \rightarrow WW, ZZ$ , we have ignored  $SU(2)_L \times U(1)_Y$  anomaly, since these couplings are allowed at the tree level already, unlike the  $\phi - g - g$  or  $\phi - \gamma - \gamma$  couplings. This should be a good approximation for a relatively light radion.

Using the above results, we show the decay rate of the radion and the relevant branching ratio for each channel available for a given  $m_\phi$  in Figs. 1 and 2. In the numerical analysis, we use  $\Lambda_\phi = v = 246$  GeV and  $m_h = 150$  GeV, and also included the QCD corrections. The decay rates for different values of  $\Lambda_\phi$  can be obtained through the following scaling :  $\Gamma(\Lambda_\phi) = (v/\Lambda_\phi)^2 \Gamma(\Lambda_\phi = v)$ . The decay rate scales as  $(v/\Lambda_\phi)^2$ , but the branching ratios are independent of  $\Lambda_\phi$ . In Fig. 1, we also show the decay rate of the SM Higgs boson with the same mass as  $\phi$ . We note that the light radion with  $\Lambda_\phi = v$  could be a much broader resonance compared to the SM Higgs even if  $m_\phi \lesssim 2m_W$ . This is because the dominant decay mode is  $\phi \rightarrow gg$  (see Fig. 2), unlike the SM Higgs for which the  $b\bar{b}$  final state is a dominant decay mode. This phenomenon is purely a quantum field theoretical effect : enhanced  $\phi - g - g$  coupling due to the trace anomaly. For a heavier radion, it turns out that  $\phi \rightarrow VV$  with  $V = W$  or  $Z$  dominates other decay modes once it is kinematically

allowed. Also the branching ratio for  $\phi \rightarrow hh$  can be also appreciable if it is kinematically allowed. This is one of the places where the difference between the SM and the radion comes in. If  $\Lambda_\phi \gg v$ , the radion would be a narrow resonance and should be easily observed as a peak in the two jets or  $WW(ZZ)$  final states. Especially  $\phi \rightarrow ZZ \rightarrow (l\bar{l})(l'\bar{l}')$  will be a gold plated mode for detecting the radion as in the case of the SM Higgs. Even in this channel, one can easily distinguish the radion from the SM Higgs by difference in their decay width.

The perturbative unitarity can be violated (as in the SM) in the  $V_L V_L \rightarrow V_L V_L$  or  $hh \rightarrow hh$ , etc. Here we consider  $hh \rightarrow hh$ , since the  $\phi - h - h$  coupling scales like  $s/\Lambda_\phi$  for large  $s \equiv (p_{h_1} + p_{h_2})^2$ . The tree-level amplitude for this process is

$$\begin{aligned} \mathcal{M}(hh \rightarrow hh) = & -\frac{1}{\Lambda_\phi^2} \left( \frac{s^2}{s - m_\phi^2} + \frac{t^2}{t - m_\phi^2} + \frac{u^2}{u - m_\phi^2} \right) \\ & -36\lambda^2 v^2 \left( \frac{1}{s - m_h^2} + \frac{1}{t - m_h^2} + \frac{1}{u - m_h^2} \right) \\ & -6\lambda, \end{aligned} \quad (8)$$

where  $\lambda$  is the Higgs quartic coupling, and  $s + t + u = 4m_h^2$ . Projecting out the  $J = 0$  partial wave component ( $a_0$ ) and imposing the partial wave unitarity condition  $|a_0|^2 \leq \text{Im}(a_0)$  (i.e.  $|\text{Re}(a_0)| \leq 1/2$ ), we get the following relation among  $m_h, v, m_\phi$  and  $\Lambda_\phi$ , for  $s \gg m_h^2, m_\phi^2$ :

$$\left| \frac{2m_h^2 + m_\phi^2}{8\pi\Lambda_\phi^2} + \frac{3\lambda}{8\pi} \right| \leq \frac{1}{2}. \quad (9)$$

This bound is shown in the lower three curves of Fig. 3. We note that the perturbative unitarity is broken for relatively small  $\Lambda_\phi \lesssim 130(300)$  GeV for  $m_\phi \sim 200$  GeV (1 TeV). Therefore, the tree level results should be taken with care for this range of  $\Lambda_\phi$  for a given radion mass.

At the  $e^+e^-$  colliders, the main production mechanism for the radion  $\phi$  is the same as the SM Higgs boson : the radion-strahlung from  $Z$  and the  $WW$  fusion, the latter of which becomes dominant for a larger CM energy [7]. Again we neglect the anomaly contributions here. Since both of these processes are given by the rescaling of the SM Higgs production rates, we can use the current search limits on Higgs boson to get the bounds on radion. With the data from L3 collaboration [8], we show the constraints of  $\Lambda_\phi$  and  $m_\phi$  in the left

three curves of Fig. 3. Since L3 data is for  $\sqrt{s} = 189$  GeV and mass of  $Z$  boson is about 91 GeV, the allowed energy for a scalar particle is about 98 GeV. If the mass of the scalar particle is larger than 98 GeV, then the cross section vanishes. Therefore if  $m_\phi$  is larger than 98 GeV, there is no constraint on  $\Lambda_\phi$ . And the forbidden region in the  $m_\phi - \Lambda_\phi$  plane is not changed by  $m_h \gtrsim 98$  GeV, because there is no Higgs contribution to the constraint for  $m_h \gtrsim 98$  GeV.

The radion production cross sections at NLC's and the corresponding constant production cross section curves in the  $(\Lambda_\phi, m_\phi)$  plane are shown in Fig. 4 and Fig. 5, respectively. We have chosen three different CM energies for NLC's :  $\sqrt{s} = 500$  GeV, 700 GeV and 1 TeV. We observe that the relatively light radion ( $m_\phi \lesssim 500$  GeV) with  $\Lambda_\phi \sim v$  (upto  $\sim 1$  TeV) could be probed at NLC's if one can achieve high enough luminosity, since the production cross section in this region is less than a picobarn.

The production cross sections of the radion at hadron colliders are given by the gluon fusion into the radion through quark loop diagrams, as in the case of Higgs boson production, and also through the trace anomaly term, Eq. (4), which is not present in the case of the SM Higgs boson :

$$\sigma(pp \text{ (or } p\bar{p})) = K \hat{\sigma}_{\text{LO}}(gg \rightarrow \phi) \int_\tau^1 \frac{\tau}{x} g(x, Q^2) g(\tau/x, Q^2) dx, \quad (10)$$

where  $\tau \equiv m_\phi^2/s$  and  $\sqrt{s}$  is the CM energy of the hadron colliders ( $\sqrt{s} = 2$  TeV and 14 TeV for the Tevatron and LHC, respectively). The  $K$  factor includes the QCD corrections, and we set  $K = 1.5$ . The parton level cross section for  $gg \rightarrow \phi$  is given by

$$\hat{\sigma}_{\text{LO}}(gg \rightarrow \phi) = \frac{\alpha_s^2(Q)}{256\pi\Lambda_\phi^2} \left| b_{QCD} + \sum_q I_q(x_q) \right|^2, \quad (11)$$

where  $I(z)$  is given in the Eqs. (7). For the gluon distribution function, we use the CTEQ5L parton distribution functions [9]. In Fig. 6, we show the radion production cross sections at the Tevatron and LHC as functions of  $m_\phi$  for  $\Lambda_\phi = v$ . We set the renormalization scale  $Q = m_\phi$  as shown in the figure. When we vary the scale  $Q$  between  $m_\phi/2$  and  $2m_\phi$ , the production cross section changes about +30% to -20%. The production cross section will

scale as  $(v/\Lambda_\phi)^2$  as before. Compared to the SM Higgs boson productions, one can clearly observe that the trace anomaly can enhance the hadroproduction of a radion enormously. As in the SM Higgs boson, there is a great possibility to observe the radion upto mass  $\sim 1$  TeV if  $\Lambda_\phi \sim v$ . For a smaller  $\Lambda_\phi$ , the cross section becomes larger but the radion becomes very broader and it becomes more difficult to find such a scalar. For a larger  $\Lambda_\phi$ , the situation becomes reversed : the smaller production cross section, but a narrower width resonance, which is easier to detect. In any case, however, one has to keep in mind that the perturbative unitarity may be violated in the low  $\Lambda_\phi$  region.

In summary, we presented the collider phenomenology for the radion, which was suggested by means of stabilizing the modulus in Randall-Sundrum scenario. Unlike other similar scenarios solving the hierarchy problem where the radion or Kaluza-Klein modes are heavy and/or very weakly coupled to the SM fields, the radion discussed by Goldberger and Wise can have sizable interactions with the SM, only suppressed by a one power of the electroweak scale. The radion phenomenology is very similar to the SM Higgs boson upto a simple rescaling of couplings by  $v/\Lambda_\phi$ , except that its couplings to two gluons or two photons are enhanced by the trace anomaly. Also  $\phi - h - h$  coupling can be substantially larger than the corresponding triple Higgs couplings, and it increases as  $m_\phi$  or the CM energy grows up. We discussed various branching ratios and the decay rate of this radion, and the possibility to discover it at linear or hadron colliders. Unlike the SM Higgs boson, the relatively light radion dominantly decays into two gluons, not into the  $b\bar{b}$  pair, and this makes the radion substantially broader than the SM Higgs if  $\Lambda_\phi = v$ . A heavier radion decays into  $WW, ZZ$  pairs with some fraction into two Higgs if it is kinematically allowed. Depending on the  $\Lambda_\phi$ , the radion can be either broad or narrow, leading to larger (smaller) production rates at hadron colliders but more harder (easier) to detectability. One may be also able to probe some regions of  $(m_\phi, \Lambda_\phi)$  if enough luminosity is achieved. It would be exciting to search for such a scalar particle which interacts with the trace of the energy-momentum tensor of the SM at the current/future colliders. Finally, although we considered the radion in the Randall-Sundrum-Goldberger-Wise scenario, our study can be equally applied to any scalar



particle which couples to the  $T_\mu^\mu(\text{SM})$ .

### ACKNOWLEDGMENTS

The work of SB, PK and HSL was supported by grant No. 1999-2-111-002-5 from the interdisciplinary Research program of the KOSEF and BK21 project of the Ministry of Education. JL is supported by the Alexander von Humboldt Foundation.

*Notes Added :* While we were completing this work, there appeared two papers [10] [11] that consider the same subjects as we do. The paper by Giudice *et al.* includes a direct coupling between the radion and the Ricci scalar parameterized by  $\xi$  :  $\mathcal{L}_{\text{int}} = -\xi R\phi^2/2$ . Our case corresponds to  $\xi = 0$  in Ref. [10]. And the usefulness of the mode  $\phi \rightarrow \gamma\gamma$  at hadron colliders was emphasized in Ref. [11]. Qualitative conclusions of these papers are the same as ours where there are overlaps.

# FIGURES

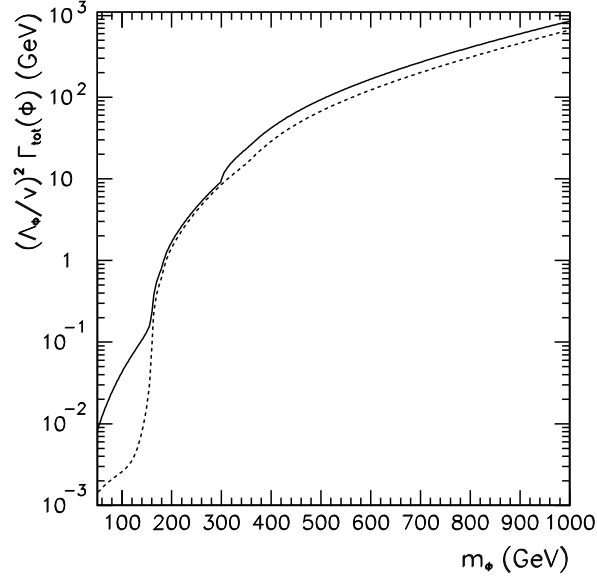


FIG. 1. The total decay rate (in GeV) for the radion  $\phi$  for  $m_h=150$  GeV with a scale factor  $(\Lambda_\phi/v)^2$ . The decay rate of the SM Higgs boson is shown in the dashed curve for comparison.

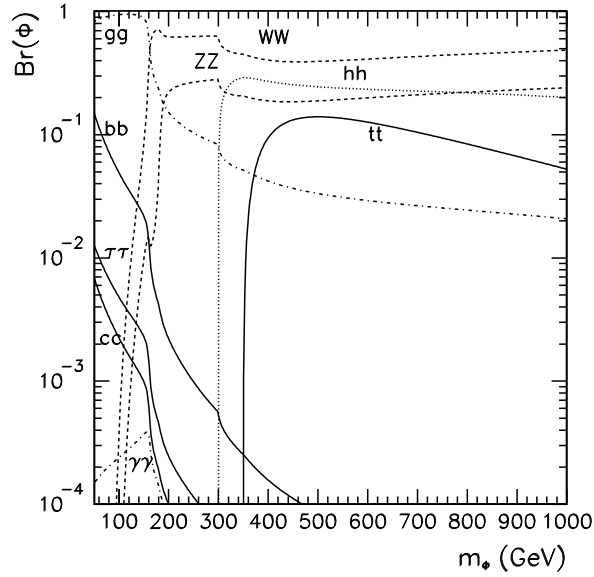


FIG. 2. The branching ratios for the radion  $\phi$  into the SM particles.

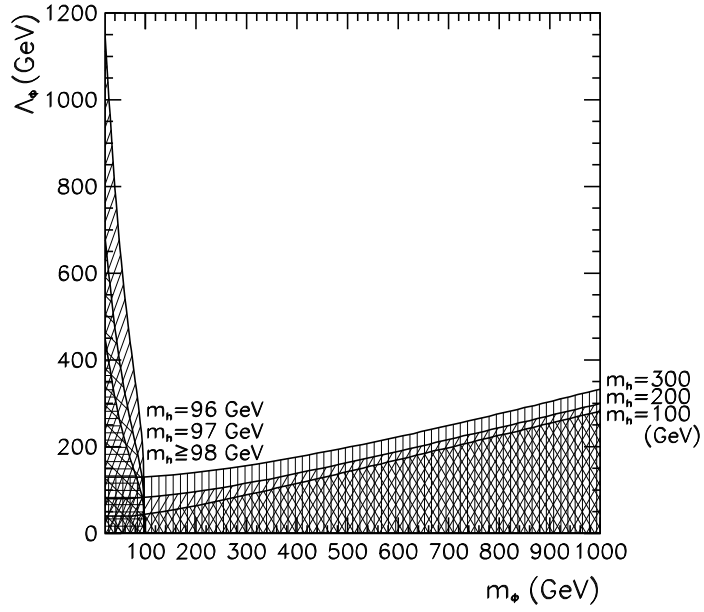


FIG. 3. The excluded region in the  $m_\phi$  and  $\Lambda_\phi$  space obtained from the recent L3 result on the SM Higgs search (the left three curves) and perturbative unitarity bound (the lower three curves).

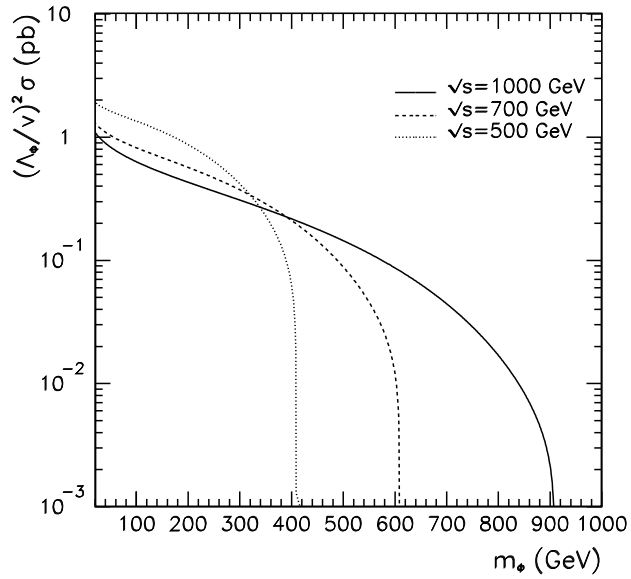


FIG. 4. The production cross section for the radion at NLC's at  $\sqrt{s} = 500$  , 700 and 1000 GeV, respectively.

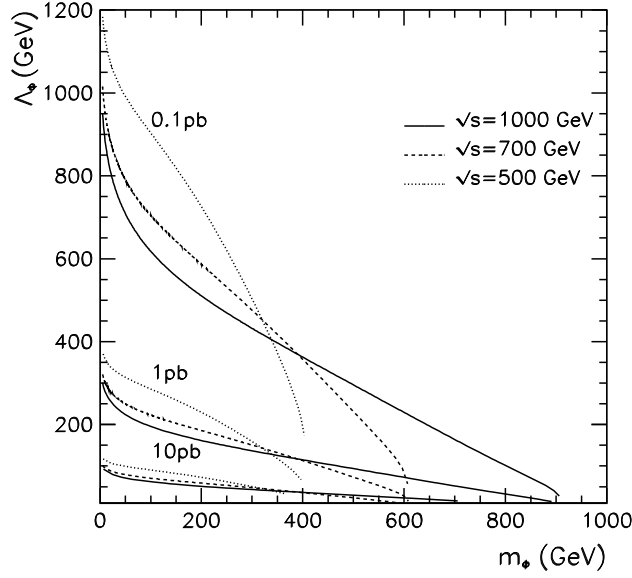


FIG. 5. The constant radion production cross section curves at next linear colliders (NLC's) for  $\sqrt{s} = 500, 700$  and  $1000$  GeV

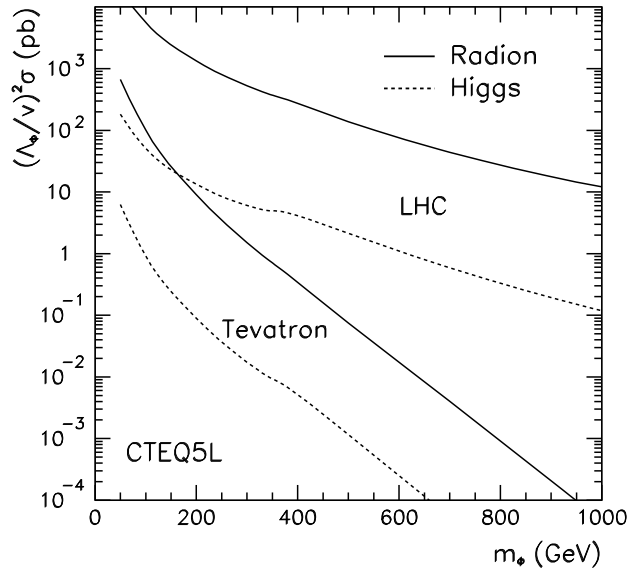


FIG. 6. The radion production cross section via gluon fusions at the Tevatron ( $\sqrt{s} = 2$  TeV) and LHC ( $\sqrt{s} = 14$  TeV) with a scale factor  $(\Lambda_\phi/v)^2$ . The Higgs production cross sections are shown in dashed curves for comparison.

## REFERENCES

- [1] L. Randall and R. Sundrum, Phys. Rev. Lett. **83**, 3370 (1999); Phys. Rev. Lett. **83**, 4690 (1999).
- [2] W.D. Goldberger and M.B. Wise, Phys. Rev. Lett. **83**, 4922 (1999).
- [3] W.D. Goldberger and M.B. Wise, hep-ph/9911457.
- [4] C. Csáki, M. Graesser, L. Randall and J. Terning, hep-ph/9911406.
- [5] U. Mahanta, S. Rakshit, hep-ph/0002049.
- [6] R. Crewther, Phys. Rev. Lett. **28**, 1421 (1972) ; M. Chanowitz and J. Ellis, Phys. Lett. **40 B**, 397 (1972) ; Phys. Rev. **D 7**, 2490 (1973) ; J. Collins, L. Duncan and S. Joglekar, Phys. Rev. **D 16**, 438 (1977).
- [7] E. Accomando *et al.*, Phys. Rep. **299**, 1 (1998).
- [8] L3 Collaboration, hep-ex/9909004.
- [9] H.L. Lai *et al.* (CTEQ Collaboration), Eur.Phys.J. **C 12** 375 (2000).
- [10] G. F. Giudice, R. Rattazzi and J. D. Wells, CERN-TH/2000-051, SNS-PH/2000-03, UCD-20007, LBNL-45301, hep-ph/0002178.
- [11] U. Mahanta and A. Datta, hep-ph/0002183.